Published in final edited form as:
Bioconjug Chem. 2010 September 15; 21(9): 1656–1661. doi:10.1021/bc1001664.

Liposomal Formulation of Amphiphilic Fullerene Antioxidants

Zhiguo Zhou[*], **Robert P. Lenk**, **Anthony Dellinger**, **Stephen R. Wilson**, **Robert Sadler**, and **Christopher L. Kepley**
Luna nanoWorks, a division of Luna Innovations Incorporated, 521 Bridge Street, Danville VA 24541

Abstract

Novel amphiphilic fullerene[70] derivatives that are rationally designed to intercalate in lipid bilayers are reported, as well as its vesicular formulation with surprisingly high loading capacity up to 65% by weight. The amphiphilic C_{70} bisadduct forms uniform and dimensionally stable liposomes with auxiliary natural phospholipids as demonstrated by buoyant density test, particle size distribution and ^{31}P NMR. The antioxidant property of fullerenes is retained in the bipolarly functionalized C_{70} derivative, Amphiphilic Liposomal Malonylfullerene[70] (ALM) as well as in its liposomal formulations, as shown by both electron paramagnetic resonance (EPR) studies and *in vitro* reactive oxygen species (ROS) inhibition experiments. The liposomally formulated ALM efficiently quenched hydroxyl radicals and superoxide radicals. In addition, the fullerene liposome inhibited radical-induced lipid peroxidation and maintained the integrity of the lipid bilayer structure. This new class of liposomally formulated, amphipathic fullerene compounds represents a novel drug delivery system for fullerenes and provides a promising pathway to treat oxidative stress-related diseases.

INTRODUCTION

Fullerenes and their derivatives have been proposed as free radical scavengers (1), and a number of investigations have studied fullerene (C_{60}) derivatives as potential free radical antioxidant therapeutics (2–5). Fullerenes (both pristine and derivatized fullerenes) have a tendency toward aggregation in aqueous environments making them unsuitable for therapeutic applications. For example, formulation techniques for preparing fullerene-based therapeutic candidates include host-guest complexation with cyclodextrins and calixerenes, surfactant solubilization with Tween-20 and polyvinylpyrrolidone (PVP), etc. These preparations have their respective limitations in terms of uniformity of formulation, loading capacity, aggregation and partition coefficient (5). Derivatization of fullerenes by directly adding moieties to the carbon cage has been used as a strategy to produce useful drug candidates. Such fullerene compounds including polyhydroxylated C_{60} (fullerenol) (6–7), polysulfonated C_{60} (8), carboxylated fullerenes (9–10) have been shown to block free radical damages in several oxidative stress-related diseases including ischemia/reperfusion injury, inflammatory apoptosis, and neurogenerative diseases. However, aggregation in aqueous media to form particles with a broad range of diameter distributions is a general problem for many of those compounds (11). Poly-derivatized fullerenes are often a mixture of many compounds, poorly characterized and not suitable for pharmaceutical development. In addition, it has been shown that cytotoxicity of fullerenes is related to the degree of cage

[*]Corresponding author: Zhiguo Zhou, Luna nanoWorks, a division of Luna Innovations Incorporated, 521 Bridge Street, Danville VA 24541; zhouz@lunainnovations.com; Phone: 434-483-4234; Fax: 434-483-4195.

SUPPORTING INFORMATION AVAILABLE: Additional information as described in the text and mass spectra. This material is available free of charge via the Internet http://www.acs.org.

derivatization, water solubility, aggregation and particle size (11). An alternative approach in which fullerenes are encapsulated in bilayer vesicles such as liposomes has been proposed to overcome these limitations. Bensasson described the preparation of vesicles by incorporating C_{60} into L-α-phophatidyl cxholine purified from egg yolk (Egg-PC) (12). However, the authors reported that only 3% or less C_{60} was incorporated in Egg-PC liposomes and the preparation was not uniformly reproducible. Incorporation of C_{60} into L-α-phophatidyl ethanolamine (PE) was limited to 7% (13). Fullerene liposomes have also been prepared by transferring fullerenes from their water soluble host-guest complexes (C_{60}·γ-CD and C_{70}·γ-CD) to lipid membranes for photodynamic therapy (PDT) (14–15). The limited number of reports on liposomal fullerene formulations was all intended to use underivatized fullerenes that are not lipophilic, rather aromatic, and structurally incompatible with natural phospholipids, therefore the fullerene contents were low and their dimensional stabilities were problematic. Further, the loading capacity of lipophilic drugs physically entrapped in liposome bilayer is limited due to the membrane destabilization effect. Thus, it is necessary to develop new drug delivery strategies that can efficiently deliver fullerenes for therapeutic applications.

Given the low contents of pristine fullerenes in liposomal formulations, we hypothesized that incorporating amphiphilic fullerenes in vesicles would greatly increase their ability to be intercalated within the lipid bilayers. Herein, we report the design and synthesis of this new class of amphiphilic fullerenes, their liposome formulation and biological activities as radical scavengers. A key to obtaining a uniform vesicular preparation with high fullerene content and dimensional stability is to incorporate amphiphilic fullerene derivatives which mimic the structure of natural phospholipids. Hirsch has reported amphiphilic C_{60} derivatives in which multiple aliphatic hydrocarbons were attached at various sites on the fullerene cage (16–17). However these “buckysomes” don’t assemble into stable bilayers readily and the addition of multiple groups could significantly damage its bioactivities.

Figure 1 illustrates the design strategy in which the amphiphilic fullerenes and phospholipids are hypothesized to coassemble and form bilayer vesicles. As shown below, this method leads to highly increased loading capacity of fullerenes. The amphiphilic fullerene compounds don’t form bilayer vesicles by themselves, but require membrane-forming lipids with lipid-to-fullerene molar ratio greater than 1:1 in order to produce uniform and dimensionally stable vesicles. We have also discovered that the oval structure of C_{70} molecule (as opposed to the spherical C_{60}) provides a novel structural platform to prepare this new type of amphiphilic fullerenes. C_{70} has two reactive poles and a relatively inert equatorial region and this allows for sequentially attaching lipophilic and hydrophilic groups at the two poles, respectively (18). The large underivatized zone around the C_{70} belt has very high radical reactivity due to the significant orbital overlap of its lowest unoccupied molecular orbital (LUMO) and highest occupied molecular orbital (HOMO) that is expected for sites of maximum). radical reactivity (19–21 The fullerene-enriched liposome provides a novel formulation approach that not only enhances the fullerene delivery efficiency but also maintain their antioxidative properties.

MATERIALS AND METHODS

Synthesis of C_{70} Monoadduct 2

To a stirred solution of C_{70} (84.0 mg, 0.1 mmol), didodeceylmalonate **1** (44.0 mg, 0.1 mmol) prepared using literature procedure (22), and iodine (25.4 mg, 0.1 mmol) in 60 mL of dry toluene was added dropwise a solution of DBU (38.0 mg, 0.25 mmol) in 5 mL of dry toluene under nitrogen at room temperature. Upon completion of addition, the reaction mixture was stirred for additional 3 hours. The reaction mixture was then washed with brine and dried over anhydrous $MgSO_4$. The raw mixture was subjected to flash chromatography

on silica gel. Unreacted C_{70} was removed by eluting the column with a mixture of toluene and hexanes (60/40, v/v), and then the eluant was changed to toluene/hexanes (90/10, v/v) to give the product **2** (108 mg, 85%). The undesirable bisadducts were eluted from the column with DCM. MALDI-MS: 1278.4, ^{1}H NMR (CDCl3): δ 0.79 (6H, t), 1.20 (32H, m), 1.38 (4H, m), 1.75 (4H, m), 4.37 (4H, t); ^{13}C NMR (CDCl3) δ 14.5, 22.3, 25.8, 28.7, 29.1, 29.2, 29.3, 29.8 (3×), 31.9, 37.2, 67.0, 130.7, 130.8, 130.9, 132.8, 133.6, 137.0, 140.7, 141.6, 142.2, 142.8, 143.0, 143.5, 143.8, 143.9, 144.9, 145.9, 146.0, 146.5, 147.0, 147.3, 147.5, 147.6, 148.4, 148.5, 148.6, 148.8, 149.1, 149.3, 149.4, 150.6, 150.8, 151.2, 151.3, 151.4, 155.1, 163.5.

Synthesis of Di(*tert*-butylglycolate)malonate 3

To a stirred solution of malonic acid (1.04 g, 10 mmol) in 60 mL 1,4-dioxane was added 2.78 mL of TEA (2.02 g, 20 mmol). The mixture was stirred for 15 minutes before *tert*-butyl bromoacetate (4.68 g, 24 mmol) was added dropwise. The resulting mixture was vigorously stirred for 2–3 days until the reaction was complete as monitored by TLC. The precipitates were then filtered and the filtrate was washed twice with brine, dried over $MgSO_4$, rotavaped *in vacuo* to give the pure di(*tert*-butylglycolate)malonate **3** as a colorless oil (2.92 g, 88%). ^{1}H NMR (CDCl3): δ ppm 1.39 (18H, s), 3.51 (2H, s), 4.49 (4H, s); ^{13}C NMR (CDCl3) δ ppm 28.5, 40.2, 61.4, 82.3, 165.5, 167.3.

Synthesis of ALM

To a stirred solution of monoadduct **2** (127.8 mg, 0.1 mmol), di(tert-butylglycolate)malonate **3** (33.2 mg, 0.1 mmol), and iodine (25.4 mg, 0.1 mmol) in 60 mL of dry toluene was dropwise added a solution of DBU (35.0 mg, 0.22 mmol) in 5 mL of dry toluene under nitrogen at room temperature. The resulting reaction mixture was stirred for 6 hours. The reaction mixture was washed with brine and then dried over anhydrous $MgSO_4$. The raw mixture was subjected to flash chromatography on silica gel. Unreacted monoadduct was removed by eluting the column with toluene, and then the eluant was changed to DCM to give the product (121 mg, 75%). MALDI-MS: 1608.2, ^{1}H NMR (CDCl3): δ 0.75 (6H, m), 1.19 (32H, m), 1.38 (4H, m), 1.43 (18H, s), 1.71 (4H, m), 4.39 (4H, m), 4.75 (4H, m). The product diester (80.0 mg) was dissolved in a mixture of 30 mL DCM and 9 mL TFA, and stirred for 2 hours. The solvent was evaporated and dried under vacuum to quantitatively yield pure ALM. MALDI-MS: 1498.2 (see MALDI-MS spectra in SI), ^{1}H NMR (DMSO): δ 0.79 (6H, m), 1.21 (32H, m), 1.39 (4H, m), 1.74 (4H, m), 4.40 (4H, m), 4.78 (4H, m).

Liposome Preparation

Two parts (by weight) of egg-PC or other lipids such as DMPC and DSPC were added to one part amphipathic ALM in diethyl ether (1mg/mL). The addition of lipids enhanced the solubility of ALM, although ALM itself has reasonable solubility in diethyl ether. The mixture was sonicated for 2 minutes before filtered via 0.2 μm filter. To the filtrate an aqueous buffered solution (PBS, phosphate buffered saline, pH = 7.4) was added, and the two phase mixture was sonicated in a bath sonicator while purging with nitrogen to produce oligolamellar vesicles. Those oligolamellar vesicles were extruded with nucleopore membranes of 0.4 μm, 0.2 μm and 0.1 μm, twice each pore size. The final ALM concentration in liposome suspensions was determined by UV-Vis spectroscopy with a standard curve after extracting it to organic solvents. Size distribution of extruded liposomes was measured by dynamic light scattering (DLS) with Zetasizer nano S90.

Inhibition of Lipid Peroxidation

Dye-encapsulated liposomes were prepared by adding a buffered solution of the dye HPTS (20 mM, pH = 6.6) to an ether solution of egg-PC lipids (1 mg/mL) with or without ALM

(1% by weight), purging nitrogen to remove ether in a bath ultrasonicator at room temperature, and extruding the crude liposomes with 400, 200 and 100 nm nuclear-pore membranes twice each. Dye-encapsulated liposome materials were separated from free dyes by SEC (size exclusion chromatography) on a Sephadex G-50 column with a buffered solution (pH = 7.8) (23–24). The final dye concentration was 0.2 mM as determined by its UV-Vis absorption. The absorption spectrum of the purified dye-encapsulated liposome samples were taken before and after the addition of Fenton reagents, and the final concentrations of H_2O_2 and $FeSO_4$ are 1 mM and 0.05 mM, respectively. Each scan was recorded at 30 min, 1 hr, 2 hr, 4 hr, 8 hr, 16 hr, 24hr, 32 hr and 48 hr after the radical initiation. The absorbance ratio (A_{450nm}/A_{405nm}) and absorbance difference (A_{450nm}-A_{405nm}) were plotted as the function of reaction time.

EPR Experiments

EPR studies on radical quenching (hydroxyl radicals and superoxide radicals) were performed as described (25). Compound ALM was dissolved in dry DMSO at 1.0 mg/mL (0.67mM) and DMSO was run as a vesicle control. Hydroxyl radicals were generated using standard concentrations of Fe^{2+}/H_2O_2 through Fenton reactions. Superoxide radical anions $O_2\cdot^-$ were generated through xanthine oxidase metabolism of hypoxanthine (HX/XO). EPR signals were acquired after 20 minutes incubation of ALM with radical-generating systems.

Cellular ROS Inhibition

U937 monocyte cells obtained from ATCC (Manassas, VA) were cultured in RPMI-1640 media supplemented with 10% FBS (fetal bovine serum). Cells were pretreated with ALM liposome, control liposome or untreated overnight in a 37°C incubator with 6% CO_2, washed, and resuspended in RPMI medium containing 5 μM DCFH-DA (2',7'-dichlorodihydrofluorescein diacetate) at 37°C for 30 minutes. After incubation the cells were washed (to remove any excess DCFH-DA) and activated with 10 μg/ml LPS (lipopolysaccharide). Activation-induced changes in mean fluorescence were measured real time using a Perkin Elmer LS55 Spectrofluorometer with excitation at 502 nm and emission at 523 nm for 15 minutes. The data are presented as fluorescence intensity of the 523 nm emission over time. All experiments were performed in triplicate. The ROS inhibition was defined as the percentage of the loss of DCF fluorescence when treated with liposome samples relative to the fluorescence intensity of untreated ones. Separate experiments were performed to ensure that the liposomal fullerenes do not interfere with the indicator dye in terms of the intensity of fluorescent signals.

RESULTS AND DISCUSSIONS

Synthesis

Scheme 1 shows the synthesis of amphiphilic C_{70} compound ALM. The hydrophilic and hydrophobic groups are introduced to C_{70} through two-step cyclopropanation reactions of respective malonates under typical Bingel-Hirsch conditions in high yield (26–27). Di(*tert*-butylglycolate)malonate **3** was prepared from malonic acid and *tert*-butylbromoacetate in the presence of TEA (triethylamine) in 1,4-dioxane at room temperature for 2–3 days. After solvents were evaporated, two phase extraction (water and chloroform) yielded pure compound **3** in 85% yield. C_{70} monoadduct **2** was synthesized in 80% yield by reacting C_{70} and didodecylmalonate **1**, and purified with silica gel column. Compound **2** then underwent the second cyclopropanation reaction with malonate **3** to produce the protected precursor of ALM, which was subsequently treated with 30% TFA (trifluoroacetic acid) in DCM to deprotect the *tert*-butyl esters and produce the amphiphilic compound ALM (22). Both ALM and its *tert*-butyl ester precursor were fully characterized by NMR, MALDI-MS, FT-IR and UV-Vis absorption spectroscopy. In addition, we have demonstrated that the three

regioisomers of the C_{70} bisadduct ALM could be separated by reverse phase HPLC (0.1% TFA in ethanol, C6-phenyl column, Supporting Information Figure S1), and the structure of each of the three peaks in the HPLC chromatogram was assigned based on their polarity and distinct UV-Vis absorption in the range of 350–600 nm (18). This general synthetic approach can be used to prepare a variety of amphiphilic C_{70} compounds, simply by replacing its glycolic acid residues with other polar groups.

Liposome Preparation

ALM was first formulated in liposomes with egg-PC (L-α-phosphatidylcholine) by the reverse phase method, and the resulting suspension was extruded to obtain small vesicles (28–29). ^{31}P NMR spectroscopy confirmed the formation of bilayer liposomes and ^{31}P spectrum of ALM-PC liposome (1mg/mL ALM) shows a very sharp signal at 2.55 ppm, with a half line-width of 2.8 Hz, which is comparable to the corresponding values of liposomes made of only egg-PC (Supporting Information Figure S2) (30). The particle sizes of extruded (with 0.1 μm polycarbonate nucleopore membrane) liposomes were confirmed by DLS with an average diameter of 100 ± 20nm (31). Intriguingly, the fullerene liposomes were dimensionally very stable. The amphipathic fullerene didn't separate from the phospholipids during and after nucleopore extrusion. This was confirmed by buoyant density separation test under conditions (high-speed centrifugation at 18,000 G for 30 min.) where fullerenes not stably incorporated in bilayer membranes would separate from lipid vesicles and precipitate to the bottom of the 40% sucrose cushion. All fullerenes were found to stay on the top of sucrose solution after centrifugation, indicating that they remained tightly associated with lipids (Supporting Information Figure S3). The tight association between ALM and PC lipids was further confirmed by the observed co-elution of ALM and egg-PC on a size exclusion column. The fact that ALM only didn't form liposome and it needs the assistance of regular lipids to coassemble into liposomes also demonstrates the successful incorporation of ALM molecule in the bilayer structure formed by the auxiliary lipids (Supporting Information Figure S4). In fact, the ALM-liposome is stable for at least one year without noticeable precipitation or aggregation. The chemical stability of the fullerene compound in liposome formulations was also monitored by MALDI-MS, UV-Vis and HPLC after extracting fullerenes into organic solvents from aliquots of liposome samples, showing no decomposition or other structural changes. Next, we examined the ratio of fullerenes to lipids in the course of forming stable liposome, and found that fullerene-to-lipid molar ratio could be as high as 1:1 (or mass ratio of roughly 2:1 or 65% fullerenes). In typical preparations, the fullerene concentration is 1.0 mg/mL liposome in phosphate buffered saline. ALM was also demonstrated to form liposomes in a similar fashion with other lipids such as 1,2-dimyristoyl-sn-glycero-3-phosphocholine) (DMPC) and (1,2-distearoyl-sn-glycero-3-phosphocholine) (DSPC).

EPR Studies

Electron paramagnetic resonance (EPR) studies were conducted as described by Ali et al (25) to confirm that bipolarly functionalized C_{70} compounds were still capable of efficiently scavenging oxygen radicals (hydroxyl and superoxide radicals). Representative EPR spectra (Figure 2, insert) show typical HO· signals, as well as their quenching by ALM at four different concentrations. Figure 2 also shows the dose-response curve of hydroxyl radical-quenching by ALM solution in DMSO. As expected, ALM is a highly potent scavenger for hydroxyl radicals, significantly reducing HO· four folds at 10μg/mL (6.7uM). ALM also effectively quenched superoxide radicals at a slightly lesser extent. It is noteworthy to point out that ALM, due to its amphipathic nature, forms micelles in the assay media, and its antioxidative efficacy might be partially masked due to its limited access and interaction with free radicals generated in the media.

Protection of lipid peroxidation

When lipid molecules, especially unsaturated lipids in cell membrane, are exposed to radicals such as hydroxyl radicals, highly reactive lipid species (lipid alkyl radicals and lipid peroxy radicals) are formed and the resulting lipid peroxidation can eventually cause membrane leakage and cellular dysfunction (32). Fullerenes formulated in liposome vesicles are particularly attractive for inhibiting lipid peroxidation. The protection effects of ALM liposome on hydroxyl radical-induced lipid peroxidation were therefore evaluated. The hydroxyl radicals were generated by the Fenton reaction as described above. A pH sensitive dye 8-hydroxylpyrene-1,3,6-trisulfonic acid trisodium salt (HPTS) was encapsulated in the internal aqueous compartment of ALM-liposome and control liposome with a lower pH of 6.6 (23–24). The outer bulk aqueous phase has a higher pH of 7.9. Upon membrane leakage caused by lipid peroxidation, the dye absorption ratio A_{455nm}/A_{405nm} increases due to the rising pH, and a higher ratio A_{455nm}/A_{405nm} indicates a greater extent of membrane leakage and lipid peroxidation. Fullerenes have strong absorption in the range of 400–450 nm, thus the ALM content was kept very low at 1% to clearly monitor the spectral changes of the dye. In order to explicitly demonstrate the protection effects, both absorbance ratio (A_{455nm}/A_{405nm}) and absorbance difference (A_{455nm}-A_{405nm}) were plotted as a function of time (t = 0 when HO· generation reaction was initiated) (Figure 3). The membrane leakage in the control liposome was dramatic, but it was minimal in the ALM-liposome sample. Additional control experiments were also conducted and the A_{455nm}/A_{405nm} of HPTS was monitored in ALM-liposome or control liposome samples in the absence of the Fenton reagents. No noticeable changes in the absorption spectra of HPTS were observed for both control samples, excluding the possibility that the control liposome is inherently leakier than the ALM-encapsulated liposome. These results clearly demonstrate the strong protection effects of ALM liposome against radical-induced peroxidation and membrane leakage.

In vitro ROS Inhibition and Cytotoxicity

ALM liposome was also evaluated for its capability to quench extra cellular reactive oxygen species (ROS) release triggered by lipopolysaccharide (LPS) (33–34). The monocyte cell line U937 used in this study is clinically relevant to atherosclerosis. The generation of foam cells from activated monocytes involves ROS overproduction and is a key inflammatory process in atherosclerotic plaque buildup (35). U937 monocytes, before LPS activation were treated with a cell-permeable fluorogenic probe 2',7'-dichlorodihydrofluorescein diacetate (DCFH-DA) (36). Following LPS activation, DCFH-DA underwent cellular hydrolysis and oxidation by ROS to generate the highly fluorescent 2',7'-dichlorofluorescein (DCF). As shown in Figure 4, ALM liposome inhibited cellular ROS release while the control liposome (without ALM) did not. More than 80% ROS release was inhibited when the cells were treated with 6 μM ALM liposome samples, and even at 6 nM, the inhibition was over 20%. This suggests that the liposome formulation efficiently delivered amphiphilic fullerenes into cells and effectively exerted its anti-ROS efficacy. The liposomal ALM was also compared with a well-studied water soluble C_{60} derivative-C_3 (six carboxyl groups – three malonic acids directly attached to a C_{60} cage) in this assay (9). As shown in Figure 4, ALM was 40–70% more potent than C_3 in scavenging cellular ROS when compared at equal molar concentrations. This could be explained by the difference in their dipole moments, structural dimension and the resultant ability to intercalate in lipid bilayer and permeate cell membranes. Amphiphilic fullerene ALM has higher lipid/aqueous partition coefficient than C_3 in favor of membrane permeation in addition to the potential endocytotic uptake of ALM liposome.

Finally, the cytotoxicity of the ALM liposome was examined. A number of factors including chemical structure, surface modification, water solubility, aggregation, particle size and preparation procedures appear to have impacts on fullerene toxicities and behaviors in

biological systems (11,37). In general, well characterized fullerene derivatives with high solubility in buffer have little or no toxicities. We evaluated the cytotoxicity of ALM liposome with U937 monocytes, and ALM was found not cytotoxic to U937 cells when incubated with up to 67 μM (0.1mg/mL) of ALM for 6 days. The cell viabilities were comparable for ALM-treated, vitamin E-treated and untreated cells at all concentrations (Supporting Information Figure S5).

CONCLUSIONS

We have presented a novel fullerene delivery approach via liposomes enriched with amphiphilic C_{70} bisadducts that were designed to structurally mimic cellular membrane lipids. The choice of C_{70} along with its inherent bipolar bisaddition pattern represents a novel pathway to design amphiphilic fullerene compounds compatible for vesicular incorporation. The strong association between reported fullerenes and auxiliary lipids allow them to form dimensionally stable liposomes with as high as up to 65% (by weight) fullerene. By mimicking the structure of naturally occurring lipid molecules, this design overcomes several limitations in previously reported formulations including 1) low fullerene content of 3%–7% due to their use of underivatized C_{60} (12–13) or lipophilically functionalized C_{60} (38), structures of which are not dimensionally compatible with the polar head/lipophilic double-tail structure of lipids; and 2) damaged antioxidative bioactivity due to the multiple additions of six groups to C_{60} in an octahedral pattern where the spherical pi-electron conjugation is interrupted leading to interconnected biphenyls (16,39). As a drug delivery vehicle, the high fullerene loading capacity is very important and it is advantageous especially for *in vivo* studies such as the delivery of fullerene to its intended region of action at sufficient concentrations with lower dose volumes. The vesicularly-formulated fullerene ALM has been demonstrated as potent radical scavengers in three separate ROS-related experiment settings. In summary, this present approach provides a new way to deliver fullerenes to sites where their antioxidant properties can be exploited and provides a platform for synthesizing new fullerene-based therapeutics that not only retain their biological activity but can be delivered via liposome carriers.

Supplementary Material

Refer to Web version on PubMed Central for supplementary material.

Acknowledgments

This work was partially supported by NIH Grants 1R01GM083274-01 and 1R43HL087578-01A1 (CLK). We thank Dr. Anthony Ribeiro at Duke NMR Center for assistance in acquiring the ^{31}P NMR spectrum.

References

1. Krustic PJ, Wasserman E, Keizer PN, Morton JR, Preston KF. Radical Reactions of C_{60}. Science. 1991; 254:1183–1185. [PubMed: 17776407]
2. Partha R, Conyers JL. Biomedical applications of functionalized fullerene-based nanomaterials. Int J Nanomedicine. 2009; 4:261–275. [PubMed: 20011243]
3. Bosi S, Da Ros T, Spalluto G, Prato M. Fullerene derivatives: an attractive tool for biological applications. Eur J Med Chem. 2003; 38:913–923. [PubMed: 14642323]
4. Nakamura E, Isobe H. Functionalized fullerenes in water. The first 10 years of their chemistry, biology, and nanoscience. Acc Chem Res. 2003; 36:807–815. [PubMed: 14622027]
5. Jensen AW, Wilson SR, Schuster DI. Biological applications of fullerenes. Bioorg Med Chem. 1996; 4:767–779. [PubMed: 8818226]

6. Tsai MC, Chen YH, Chiang LY. Polyhydroxylated C_{60}, fullerenol, a novel free-radical trapper, prevented hydrogen peroxide- and cumene hydroperoxide-elicited changes in rat hippocampus in-vitro. J Pharm Pharmacol. 1997; 49:438–445. [PubMed: 9232545]
7. Husebo LO, Sitharaman B, Furukawa K, Kato T, Wilson LJ. Fullerenols revisited as stable radical anions. J Am Chem Soc. 2004; 126:12055–12064. [PubMed: 15382940]
8. Huang SS, Tsai SK, Chih CL, Chiang LY, Hsieh HM, Teng CM, Tsai MC. Neuroprotective effect of hexasulfobutylated C_{60} on rats subjected to focal cerebral ischemia. Free Radic Biol Med. 2001; 30:643–649. [PubMed: 11295362]
9. Dugan LL, Turetsky DM, Du C, Lobner D, Wheeler M, Almli CR, Shen CKF, Luh TY, Choi DW, Lin TS. Carboxyfullerenes as neuroprotective agents. Proc Natl Acad Sci USA. 1997; 94:9434–9439. [PubMed: 9256500]
10. Brettreich M, Hirsch A. A highly water-soluble dendro[60]fullerene. Tetrahedron Lett. 1998; 39:2731–2734.
11. Johnston HJ, Hutchison GR, Christensen FM, Aschberger K, Stone V. The biological mechanisms and physicochemical characteristics Responsible for driving fullerene toxicity. Toxicol Sci. 2010; 114:162–182. [PubMed: 19901017]
12. Bensasson RV, Bienvenue E, Dellinger M, Leach S, Seta PJ. C_{60} in model biological systems. A visible-UV absorption study of solvent-dependent parameters and solute aggregation. J Phys Chem. 1994; 98:3492–3496.
13. Hungerbuhler H, Guldi DM, Asmus KD. Incorporation of C_{60} into artificial lipid membranes. J Am Chem Soc. 1993; 115:3386–3390.
14. Ikeda A, Doi Y, Hashizume M, Kikuchi J, Konishi T. An extremely effective DNA photocleavage utilizing functionalized liposomes with a fullerene-enriched lipid bilayer. J Am Chem Soc. 2007; 129:4140–4141. [PubMed: 17371028]
15. Kato S, Kikuchi R, Aoshima H, Saitoh Y, Miwa N. Defensive effects of fullerene-C_{60}/liposome complex against UVA-induced intracellular reactive oxygen species generation and cell death in human skin keratinocytes HaCaT, associated with intracellular uptake and extracellular excretion of fullerene- C_{60}. J Photochem Photobiol B. 2010; 98:144–151. [PubMed: 20060738]
16. Brettreich M, Burghardt S, Bottcher C, Bayerl T, Bayerl S, Hirsch A. Globular amphiphiles: Membrane-forming hexaadducts of C_{60}. Angew Chem Int Ed. 2000; 39:1845–1848.
17. Maierhofer AP, Brettreich M, Burghardt S, Vostrowsky O, Hirsch A, Langridge S, Bayerl TM. Structure and electrostatic interaction properties of monolayers of amphiphilic molecules derived from C_{60}-fullerenes: A film balance, neutron, and infrared reflection study. Langmuir. 2000; 16:8884–8891.
18. Herrmann A, Rüttimann M, Thilgen C, Diederich A. Multiple Cyclopropanations of C_{70}. Synthesis and characterization of bis-, tris-, and tetrakis- adducts and chiroptical properties of bis-adducts with chiral addends, including a recommendation for the configurational description of fullerene derivatives with a chiral addition pattern. Helv Chim Act. 1995; 78:1673–1704.
19. Gan L, Huang S, Zhang X, Zhang A, Cheng B, Cheng H, Li X, Shang G. Fullerenes as a tert-butylperoxy radical trap, metal catalyzed reaction of tert-butyl hydroperoxide with fullerenes, and formation of the first fullerene mixed peroxides. J Am Chem Soc. 2002; 124:13384–13385. [PubMed: 12418881]
20. Birkett PR, Avent AG, Darwish AD, Kroto HW, Taylor R, Walton DRM. Formation and characterization of $C_{70}Cl_{10}$. J Chem Soc, Chem Commun. 1995:683–684.
21. Scuseria GE. The equilibrium structure of C_{70}. An ab initio Hartree-Fock study. Chem Phys Lett. 1991; 180:451–469.
22. Zhou Z, Schuster DI, Wilson SR. Selective syntheses of novel polyether fullerene multiple adducts. J Org Chem. 2003; 68:7612–7617. [PubMed: 14510532]
23. Kano K, Fendler JH. Pyranine as a sensitive pH probe for liposome interiors and surfaces. pH gradients across phospholipid vesicles. Biochim, Biophys Acta. 1978; 509:289–296. [PubMed: 26400]
24. Wang C, Tai LA, Lee DD, Kanakamma PP, Shen CKF, Luh TY, Cheng CH, Hwang KC. C_{60} and water-soluble fullerene derivatives as antioxidants against radical-initiated lipid peroxidation. J Med Chem. 1999; 42:4614–4620. [PubMed: 10579823]

25. Ali SS, Hardt JI, Quick KL, Kim-Han JS, Erlamger BF, Huang TT, Epstein CJ, Dugan LL. A biologically effective fullerene C_{60} derivative with superoxide dismutase mimetic properties. Free Radic Biol Med. 2004; 37:1191–1202. [PubMed: 15451059]
26. Bingel C. Cyclopropylation of fullerenes. Chem Ber. 1993; 126:1957–1958.
27. Zhou Z, Wilson SR. Tether-directed multiple functionalization of fullerene[60]. Curr Org Chem. 2005; 9:789–811.
28. Pidgeon C, McNeely S, Schmidt T, Johnson JE. Multilayered vesicles prepared by reverse-phase evaporation: liposome structure and optimum solute entrapment. Biochemistry. 1987; 26:17–29. [PubMed: 3828297]
29. Gruner SM, Lenk RP, Janoff AS, Ostro MJ. Novel multilayered lipid vesicles: comparison of physical characteristics of multilamellar liposomes and stable plurilamellar vesicles. Biochemistry. 1985; 24:2833–2842. [PubMed: 2990532]
30. Berden JA, Cullis PR, Hoult DI, McLaughlin AC, Radda GK, Richards RE. Frequency dependence of ^{31}P NMR linewidths in sonicated phospholipid vesicles: effects of chemical shift anisotropy. FEBS Lett. 1974; 46:55–58. [PubMed: 4425071]
31. Winterhalter M, Lasic DD. Liposome stability and formation: experimental parameters and theories on the size distribution. Chem Phys Lipids. 1993; 64:35–43. [PubMed: 8242841]
32. Niki E. Lipid peroxidation: physiological levels and dual biological effects. Free Radic Biol Med. 2009; 47:469–484. [PubMed: 19500666]
33. Stocker R, Keaney JF. Role of oxidative modifications in atherosclerosis. Physiol Rev. 2004; 84:1381–1478. [PubMed: 15383655]
34. Aviram M. Macrophage foam cell formation during early atherogenesis is determined by the balance between prooxidants and antioxidants in arterial cells and blood lipoproteins. Antioxid Redox Signal. 1999; 1:585–594. [PubMed: 11233155]
35. Schwartz CJ, Kelley JL, Nerem RM, Sprague EA, Rozek MM, Valente AJ, Edwards EH, Prasad AR, Kerbacher JJ, Logan SA. Pathophysiology of the atherogenic process. Am J Cardiol. 1989; 64:23G–30G.
36. Rosenkranz AR, Schmaldienst S, Stuhlmeier KM, Chen W, Knapp W, Zlabinger GJ. A microplate assay for the detection of oxidative products using 2',7'-dichlorofluorescin-diacetate. J Immunol Methods. 1992; 156:39–45. [PubMed: 1431161]
37. Kolosnjaj J, Szwarc H, Moussa F. Toxicity studies of fullerenes and derivatives. Adv Exp Med Biol. 2007; 620:168–180. [PubMed: 18217343]
38. Lens M, Medenica L, Citernesi U. Antioxidative capacity of C-60 (buckminsterfullerene) and newly synthesized fulleropyrrolidine derivatives encapsulated in liposomes. Biotechnol Appl Biochem. 2008; 51:135–140. [PubMed: 18257745]
39. Partha R, Lackey M, Hirsch A, Casscells SW, Conyers JL. Self assembly of amphiphilic C60 fullerene derivatives into nanoscale supramolecular structures. J Nanobiotechnology. 2007; 5:6, 1–11. [PubMed: 17683530]

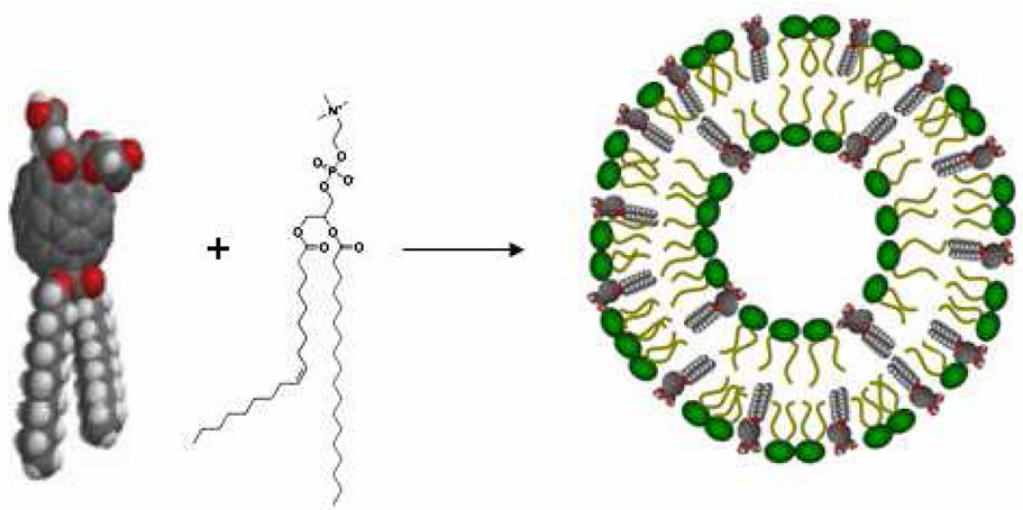

Figure 1.
Vesicle formation of amphiphilic fullerenes with auxiliary phospholipids.

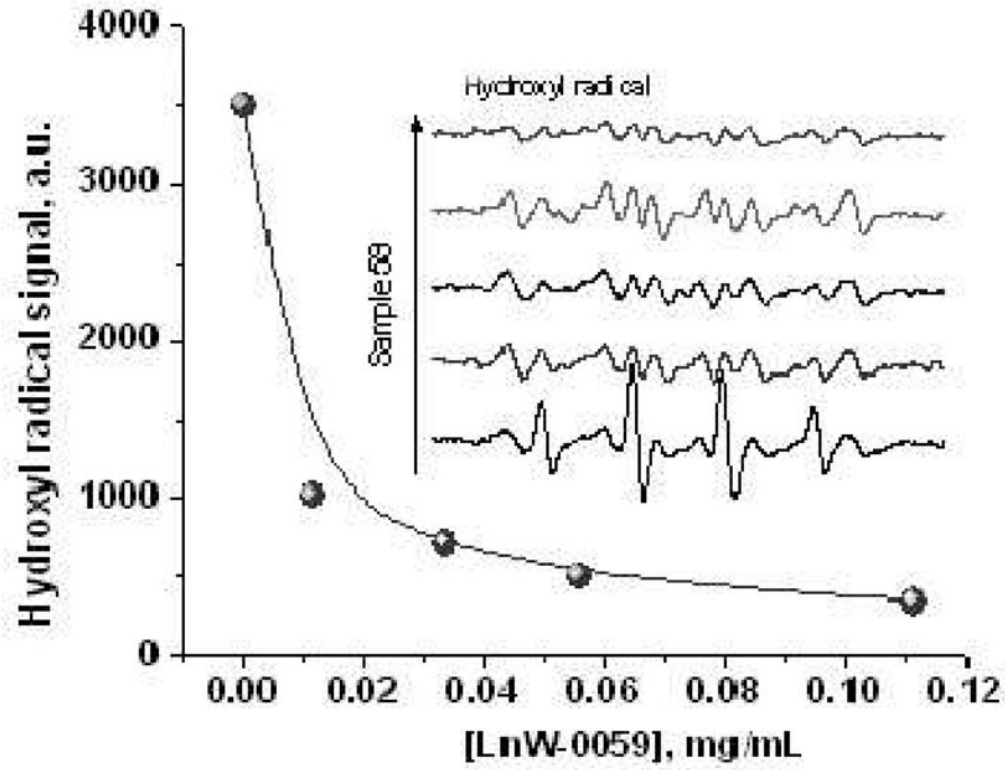

Figure 2.

Hydroxyl radical quenching by ALM at four different concentrations. Insert shows EPR spectra of hydroxyl radicals generated via the Fenton reaction, with (top 4 curves) or without (bottom curve) the addition of a DMSO solution of ALM (LnW-0059) at 0.01 mg/mL, 0.03 mg/mL, 0.05mg/mL and 0.11mg/mL. All observed signals were mixtures of DMPO-OH + DMPO-Me (Fenton products). (The DMPO-Me signal is attributable to radical reactions with DMSO).

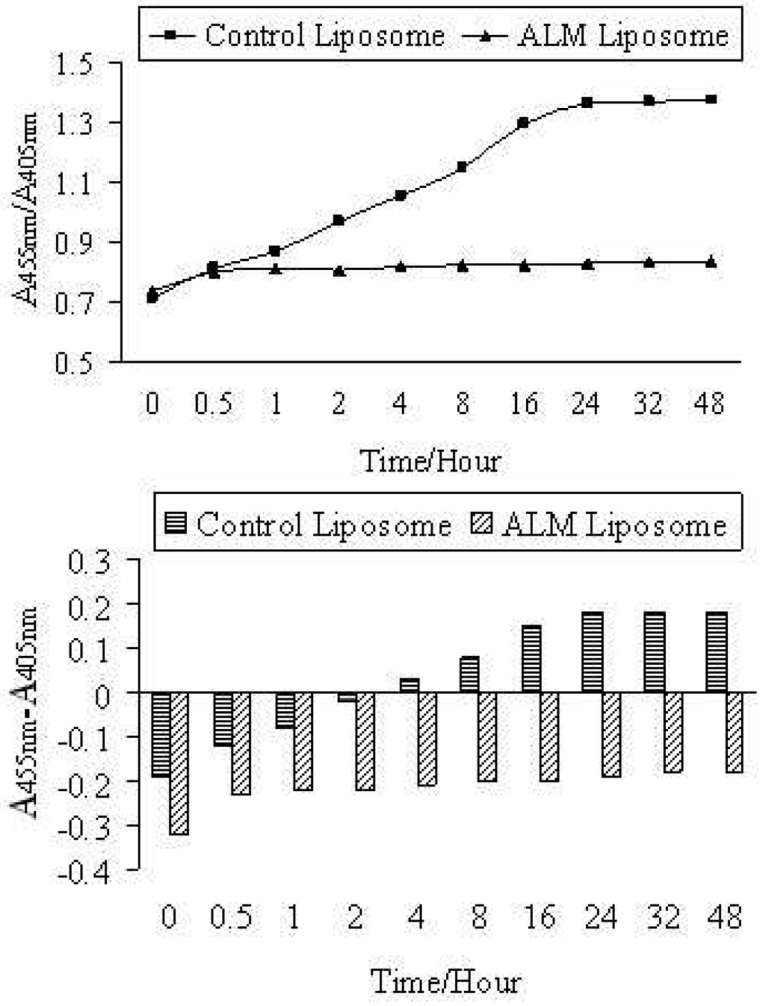

Figure 3.

Absorbance ratio (A_{455nm}/A_{405nm}, top) and absorbance difference (A_{455nm}-A_{405nm}, bottom) of HPTS as a function of reaction time from when the Fenton reagents were added to the liposome samples. 1% fullerene was contained in ALM liposome. (1.0mM H_2O_2 and 0.05mM Fe^{2+} ions of final concentrations).

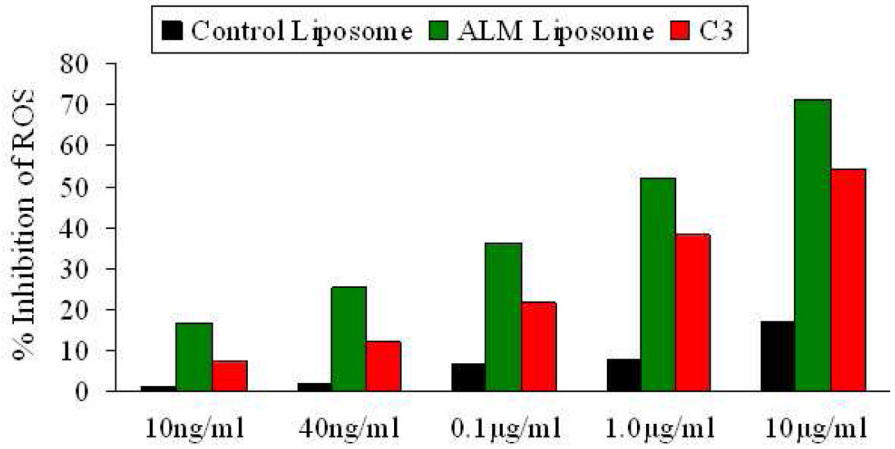

Figure 4.

Inhibition of ROS in U937 monocytes by liposomes. For each concentration, the same volume of control liposome was used as the control. The fluorescence intensity was recorded and used as the measure to quantify ROS inhibition.

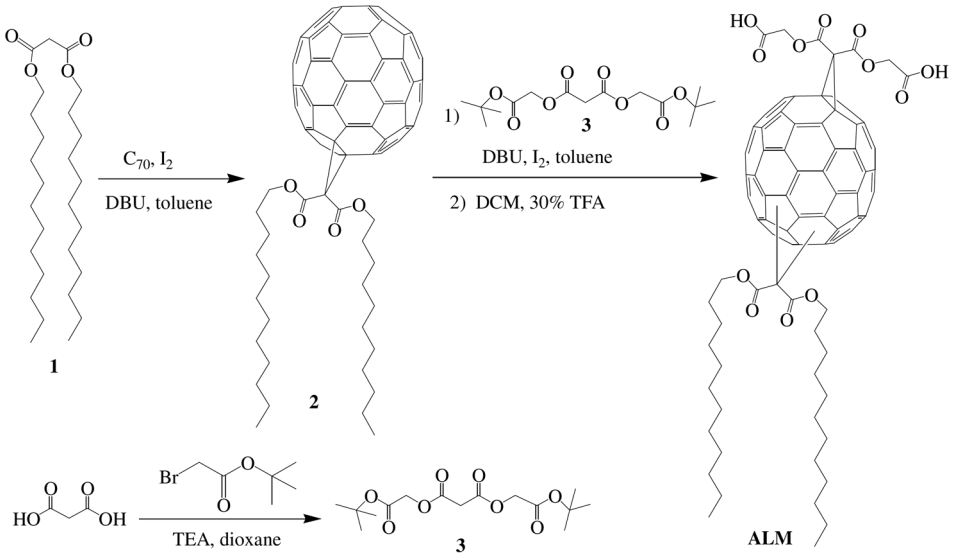

Scheme 1.
Synthesis of amphiphilic fullerene C_{70} ALM (the ALM structure represents three isomers).